

FREE SURFACE DYNAMICS OF THIN MHD SECOND-GRADE FLUID OVER A HEATED NONLINEAR STRETCHING SHEET

KIRAN KUMAR PATRA, SATYANANDA PANDA, MATHIEU SELLIER

ABSTRACT. This article presents a long-wave theory for the free surface dynamics of magnetohydrodynamics (MHD) second-grade fluid over a non-uniform heated flat elastic sheet. An evolution equation for the film thickness is derived from the instationary Navier-Stokes equations using regular asymptotic expansion with respect to the small aspect ratio of the flow domain. The derived thin film equation is solved numerically using finite volume method on a uniform grid system with implicit flux discretization. The finding reveals the dependency of the thinning behavior of the fluid film on the stretching speed and the non-Newtonian second-grade parameter.

1. INTRODUCTION

Many theoretical studies on the flow of fluid and heat transfer due to stretching sheet in the context of polymer extrusion, continuous casting, drawing of the plastic sheets, cable coating, etc., can be found in the literature, about, e.g. Newtonian fluid [2, 3, 4, 7, 8, 16, 23, 27], non-Newtonian fluid [1, 14, 21, 22] and MHD effect [13, 17, 18] as well as derivation of boundary layer equations. In general, such model reductions are based on the uniform film thickness assumption which enables the similarity transformation. Thereby the set of partial differential equations are reduced to a more tractable one of ordinary differential equations.

Recognizing the restrictions of the plane interface assumptions, Dandapat and co-workers were the first to extend the formulation to account for local deformation of the free surface in [5, 6]. The authors exploit the slenderness of the flow domain to derive a long-wave approximation of the Navier-Stokes equations and solve the resulting governing equation using the matched asymptotic method. Lately, this work was extended to include the heat transfer problem [9, 24]. In this work, the nonuniform temperature distribution at the stretching sheet induces an inhomogeneous temperature field in the film. Consequently, a surface temperature gradient develops at the film free surface. As a result of the surface tension gradients, the film thickness varies along the flow, and these deformations are advected in the stretching direction. Also, a free surface model based on a long-wave theory for

2010 *Mathematics Subject Classification.* 76A05, 76A10, 76A20, 76M12, 80A20.

Key words and phrases. Thin liquid film; heat transfer; second-grade fluid; free surface flow; magnetic field; long-wave theory.

©2017 Texas State University.

Published November 15, 2017.

the thin film dynamics of Casson fluid over a nonlinear stretching sheet including magnetic effect has been recently deduced in [26].

This work focuses on the systematic derivation, in the spirit of [9], of the thin film equation for a second-grade non-Newtonian MHD fluid over a heated steady stretching sheet without the restriction of the plane interface assumption. One motivation for this study is the flow of mucus in biological tissues which undergo expansion or contraction. A particular example is pulmonary alveoli which are covered with a lining of non-Newtonian fluid [15] and which undergo periodic expansion and contraction.

This article is organized as follows. The mathematical model for the flow of second-grade fluid is described in Sec. (2). The long-wave theory by using the standard expansion technique with respect to a small aspect ratio of the flow domain for model reduction is presented in Sec. (3). The thin film model equation is given in Sec. (4). The numerical procedure for the numerical solution of the thin film equation is explained in Sec. (5). In Sec. (6) we discuss the numerical investigation of the thin film equation, and give some conclusions from this work.

2. PHYSICAL MODEL AND PROBLEM FORMULATION

We consider here an unsteady planar fluid which lies over a heated stretching sheet in the presence of transverse magnetic field \mathbf{B}_0 as shown in Figure (1). The elastic sheet lies at $z = 0$, and the liquid-gas interface lies at $z = h(x, t)$, where the x -axis is directed along the stretching layer, and the z -axis is normal to the sheet in the outward direction toward the fluid. Gravity acts along the negative z -direction. Further, the surface at $z = 0$ starts stretching from rest and within a very short time attains the stretching velocity $u = U(x)$. The evaporation and buoyancy effects are neglected considering the liquid is non-volatile and thin. The elastic surface is heated with non-uniform temperature T_s a function of x alone, and the ambient gas phase is at constant temperature T_a . A constant uniform magnetic field of strength B_0 is applied transversely in the parallel direction to the z -axis. Since the sheet is nonconducting, an uniform electric field is applied along the z -direction to generate Lorentz force.

The fluid is assumed to be incompressible and non-Newtonian second-grade fluid with constant viscosity μ , density ρ , specific heat c_p , thermal conductivity k and the electric conductivity λ . The surface tension of the liquid-gas interface decreases linearly with temperature T according to

$$\sigma = \sigma_a(1 - \gamma(T - T_a)), \quad (2.1)$$

where σ_a is the surface tension at $T = T_a$, and $\gamma = -\frac{1}{\sigma_a} \left(\frac{d\sigma}{dT} \right)_{T=T_a}$ a positive constant specific to the fluid.

Neglecting viscous dissipation and radiation effects, the motion of the second-grade fluid due to the heated stretching sheet is governed by the continuity equation of mass flow, the momentum equation and the temperature equation.

- Continuity equation:

$$\nabla \cdot \mathbf{V} = \mathbf{0}; \quad (2.2)$$

- Momentum equation:

$$\rho \frac{D\mathbf{V}}{Dt} = \nabla \cdot \boldsymbol{\tau} + \rho \mathbf{g} + \mathbf{F}; \quad (2.3)$$

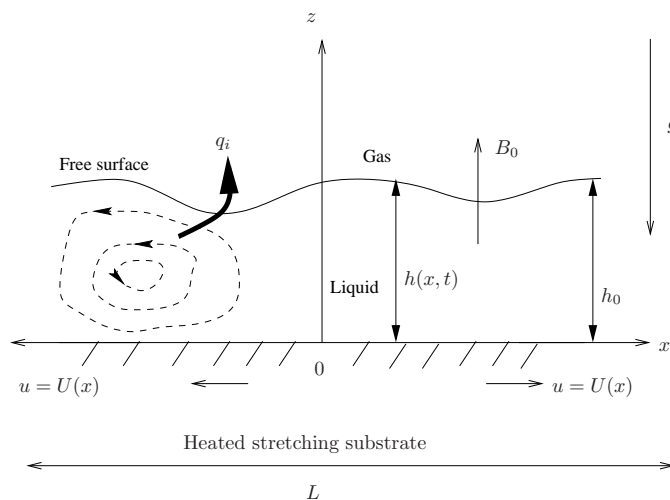


FIGURE 1. Sketch of flow geometry

- Temperature equation:

$$\rho c_p \frac{DT}{Dt} = k \nabla^2 T; \quad (2.4)$$

- Free surface boundary conditions i.e. at $z = h(x, t)$:

$$p_a + \hat{\mathbf{n}} \cdot \boldsymbol{\tau} \cdot \hat{\mathbf{n}} = -\sigma (\nabla \cdot \hat{\mathbf{n}}), \quad (2.5)$$

$$\hat{\mathbf{n}} \cdot \boldsymbol{\tau} \cdot \hat{\mathbf{t}} = \nabla \sigma \cdot \hat{\mathbf{t}}, \quad (2.6)$$

$$h_t + u h_x = w, \quad (2.7)$$

$$q_i = -k \nabla T \cdot \hat{\mathbf{n}} = \alpha (T - T_a) \quad (2.8)$$

- Boundary conditions on the stretching sheet i.e. at $z = 0$:

$$u(x, 0, t) = U(x), \quad w(x, 0, t) = 0, \quad T(x, 0, t) = T_s(x); \quad (2.9)$$

- Initial condition:

$$u(x, z, 0) = w(x, z, 0) = 0, \quad h(x, 0) = h_0 + \delta(x) \quad (2.10)$$

The symbols $\mathbf{V}(x, z, t) = (u(x, z, t), w(x, z, t))$, $\boldsymbol{\tau}$, \mathbf{g} and \mathbf{F} denote the fluid velocity at position (x, z) and time t , the Cauchy stress tensor, the acceleration due to gravity and the Lorentz force. The free surface boundary conditions are due to balance of stresses, the kinematic condition and the convective heat flux at the interface. Here, $\hat{\mathbf{n}}$ and $\hat{\mathbf{t}}$ are the unit normal and tangential vectors on the surface, respectively. The p_a stands for the atmospheric pressure at the free surface, σ is the surface tension of the fluid, q_i is the heat flux, α is the rate of heat transfer from the liquid to the ambient gas phase and the symbol ∇ stands for the gradient operator. The subscripts x and t stand for the partial differentiation with respect to x and t respectively. The symbol h_0 is the characteristic height of the free surface and δ is the initial small disturbance from h_0 .

The *Cauchy-stress tensor*, given by Rivlin and Ericksen [20] for a second-grade fluid can be written as

$$\boldsymbol{\tau} = -p\mathbf{I} + \mu\mathbf{A}_1 + \alpha_1\mathbf{A}_2 + \alpha_2\mathbf{A}_1^2, \quad (2.11)$$

where p is the pressure, \mathbf{I} is the identity tensor. The material constants α_1 and α_2 are the first and second normal stress coefficients. The quantities \mathbf{A}_1 and \mathbf{A}_2 are the first two Rivlin-Ericksen tensors and they are defined as

$$\mathbf{A}_1 = (\nabla\mathbf{V}) + (\nabla\mathbf{V})^*, \quad \mathbf{A}_2 = \frac{D}{Dt}\mathbf{A}_1 + \mathbf{A}_1 \cdot (\nabla\mathbf{V}) + (\nabla\mathbf{V})^* \cdot \mathbf{A}_1, \quad (2.12)$$

where D/Dt is the material time derivative, and the superscript $(*)$ is used for the transpose.

The constitutive model (2.11) is derived by considering second order approximation of retardation parameter. Dunn and Fosdick [10] have shown that this model equation is invariant under transformation and therefore the material constants must meet the following restriction

$$\mu \geq 0, \quad \alpha_1 \geq 0, \quad \alpha_1 + \alpha_2 = 0. \quad (2.13)$$

Fluids characterized by these restrictions (2.13) are called second-grade fluid. The fluid model represented by (2.11) with the relationship (2.13) is compatible with the hydrodynamics. The third relations of (2.13) is the consequence of satisfying the Clausis-Duhem inequality by fluid motion and a second relation arises due to the assumptions that specific Helmholtz free energy of the fluid takes its minimum value in equilibrium. The fluid satisfying model (2.11) with $\alpha_i < 0$; ($\alpha_i = 1, 2$) is termed as second-order fluid and with $\alpha_i > 0$ is termed as second-grade fluid. Although second-order fluid is obeying model (2.11) with $\alpha_1 < \alpha_2, \alpha_1 < 0$, exhibits some undesirable instability characteristic (Fosdick and Rajagopal [12]). The second order approximation is valid at low shear rate (Dunn and Rajagopal [11]).

The fluid is flowing under the environment of uniform transverse magnetic field, therefore momentum of the fluid is influenced by the Lorentz force $\mathbf{F} = \lambda(\mathbf{E} + \mathbf{V} \times \mathbf{B}_0) \times \mathbf{B}_0$, where $\mathbf{E} + \mathbf{V} \times \mathbf{B}_0$ represents the total current density with magnetic Reynolds number $R_m \ll 1$. The electric field $\mathbf{E} = \mathbf{0}$, as there is no electric current present during the fluid flow. The term $\mathbf{V} \times \mathbf{B}_0$ is the potential difference across the fluid. Using basic vector calculus the expression for Lorentz force can be calculated as follows

$$\mathbf{F} = \lambda(\mathbf{V} \times \mathbf{B}_0) \times \mathbf{B}_0 = -\lambda[\mathbf{V}(\mathbf{B}_0 \cdot \mathbf{B}_0) - \mathbf{B}_0(\mathbf{V} \cdot \mathbf{B}_0)] = -\lambda(uB_0^2, 0, 0) \quad (2.14)$$

Scaling the film thickness with the characteristic height of the flow ($h = h_0\tilde{h}$, $\delta = h_0\tilde{\delta}$), the coordinates by the characteristic length of the domain $(x, z) = L(\tilde{x}, \epsilon\tilde{z})$ and the velocity $(u, w) = (\nu/h_0\tilde{u}, \epsilon\nu/h_0\tilde{w})$, $U = (\nu/h_0)\tilde{U}$, the time $t = (h_0^2/\epsilon\nu)\tilde{t}$, the pressure with $p = p_a + (\rho\nu^2/\epsilon h_0^2)\tilde{p}$ and the temperature $T = T_a + (T_{s_0} - T_a)\tilde{T}$, where $\epsilon = h_0/L$ is the aspect ratio, $\nu = \mu/\rho$ is the kinematic viscosity of the fluid, T_{s_0} is the temperature of the sheet at the origin, and using the constitutive relation (2.11) with Eqs. (??), (2.13), and the external force (2.14), the non-dimensional form of the governing (2.2)-(2.10), after dropping the tilde symbol in explicit form are:

$$u_x + w_z = 0 \quad (2.15)$$

$$\begin{aligned}
& \epsilon(u_t + uu_x + wu_z) \\
&= -p_x + \epsilon^2 u_{xx} + u_{zz} + K(\epsilon^3 u_{xxt} + \epsilon u_{zzt} + \epsilon^3 uu_{xxx} - \epsilon uw_{zzz} \\
&\quad + \epsilon^3 u_x u_{xx} - \epsilon u_x u_{zz} + \epsilon^3 wu_{xxz} + \epsilon wu_{zzz} - 4\epsilon^3 w_x w_{zz} - 2\epsilon^5 w_x w_{xx} \\
&\quad + \epsilon^3 u_z w_{xx} - \epsilon u_z w_{zz} + 2\epsilon w_z u_{zz}) - \epsilon M^2 u, \tag{2.16}
\end{aligned}$$

$$\begin{aligned}
& \epsilon^3(w_t + uw_x + ww_z) \\
&= -p_z + \epsilon^4 w_{xx} + \epsilon^2 w_{zz} + K\epsilon(\epsilon^4 w_{xxt} + \epsilon^2 w_{zzt} + \epsilon^2 u w_{xzz} \\
&\quad + \epsilon^4 u w_{xxx} + 2\epsilon^4 u_x w_{xx} + \epsilon^2 w_x u_{zz} - \epsilon^4 w_x u_{xx} + \epsilon^2 w w_{zzz} \\
&\quad - \epsilon^4 w u_{xxx} + \epsilon^2 w_z w_{zz} - \epsilon^4 w_z w_{xx} - 4\epsilon^2 u_z u_{xx} - 2u_z u_{zz}) - \epsilon Fr, \tag{2.17}
\end{aligned}$$

$$\epsilon Pr (T_t + uT_x + wT_z) = \epsilon^2 T_{xx} + T_{zz}, \tag{2.18}$$

$$\begin{aligned}
& \epsilon S h_{xx} (1 - M_w CaT) (\epsilon^2 h_x^2 + 1)^{-1/2} \\
&= -(\epsilon^2 h_x^2 + 1)p + 2\epsilon^2 (\epsilon^2 h_x^2 u_x - \epsilon^2 h_x w_x - h_x u_z + w_z) \\
&\quad + K\epsilon^3 (2\epsilon^2 u_{tx} h_x^2 - 2\epsilon^2 h_x w_{tx} - 2h_x u_{tz} + 2w_{tz}) \\
&\quad + K\epsilon \left(\epsilon^2 h_x^2 (2\epsilon^2 uu_{xx} + 2\epsilon^2 wu_{xz} + u_z^2 - \epsilon^4 w_x^2) - 2\epsilon^2 h_x (\epsilon^2 uw_{xx} + uu_{xz} \right. \\
&\quad + \epsilon^2 ww_{xz} + wu_{zz} + \epsilon^2 u_x w_x - \epsilon^2 w_x w_z + u_z w_z - u_x u_z) \\
&\quad \left. + 2\epsilon^2 uw_{xz} + 2\epsilon^2 ww_{zz} + \epsilon^4 w_x^2 - u_z^2 \right), \tag{2.19}
\end{aligned}$$

$$\begin{aligned}
& -\epsilon M_w (T_x + h_x T_z) (1 + \epsilon^2 h_x)^{1/2} \\
&= (\epsilon^2 w_x + u_z)(1 - \epsilon^2 h_x^2) + 2\epsilon^2 h_x (w_z - u_x) + K((1 - \epsilon^2 h_x^2)(\epsilon^3 w_{tx} + \epsilon u_{tz}) \\
&\quad + 2\epsilon^3 h_x (w_{tz} - u_{tx})) + K \left((1 - \epsilon^2 h_x^2)(\epsilon^3 uu_{xx} + \epsilon uu_{xz} + \epsilon^3 ww_{xz} \right. \\
&\quad + \epsilon w_{zz} + \epsilon^3 u_x w_x - \epsilon^3 w_x w_z + \epsilon u_z w_z - \epsilon u_x u_z) + 2\epsilon h_x (\epsilon^2 uw_{xz} \\
&\quad \left. + \epsilon^2 ww_{zz} - \epsilon^2 uu_{xx} - \epsilon^2 wu_{xz} + \epsilon^4 w_x^2 - u_z^2) \right), \tag{2.20}
\end{aligned}$$

$$h_t = w - uh_x, \tag{2.21}$$

$$T_z - \epsilon^2 h_x T_x = -B (1 + \epsilon^2 h_x^2)^{1/2} T, \tag{2.22}$$

$$\text{and at } z = 0: \quad u = U(x), \quad w = 0, \quad T = \theta(x), \quad \text{where } \theta(x) = \frac{T_s - T_a}{T_{s_0} - T_a} \tag{2.23}$$

The non-dimensional parameters are the second grade parameter $K = \alpha_1/\rho h_0^2$, the Hartmann number $M = \sqrt{\lambda B_0^2 h_0 L/\rho\nu}$, the Froude number $Fr = gh_0^3/\nu^2$, and the Prandtl number $Pr = \rho c_p \nu/k$.

The symbol S stands for the non-dimensional surface tension parameter defined as $S = \epsilon^2 \sigma_a h_0/\rho\nu^2$. Here $Ca = \epsilon^2/S$, $B = \alpha h_0/k$ and $M_w = \sigma_a h_0 \gamma (T_{s_0} - T_a)/\rho\nu^2$ are the Capillary number, Biot number, and the effective Marangoni number, respectively. Equations (2.19) and (2.20) are obtained after using the expression for unit normal vector $\hat{\mathbf{n}} = (-h_x/\sqrt{1+h_x^2}, 1/\sqrt{1+h_x^2})$ and the unit tangent vector $\hat{\mathbf{t}} = (1/\sqrt{1+h_x^2}, h_x/\sqrt{1+h_x^2})$.

The initial conditions read:

$$u = 0, \quad w = 0, \quad h(x, 0) = 1 + \delta(x). \tag{2.24}$$

3. LONG-WAVE APPROXIMATION

The derivation of the one-dimensional thin film equation is based on long wave theory. The stated asymptotic analysis uses the techniques of [9] but extends it to incorporate the complex rheological effects.

For the underlying velocity and pressure variables, regular power series expansion in ϵ are set up. To obtain the equation of the thin film from the above problem, we expand the variables as follows:

$$(u, w, p) = (u_0, w_0, p_0) + \epsilon(u_1, w_1, p_1) + \epsilon^2(u_2, w_2, p_2) + \dots \quad (3.1)$$

Then the temperature variable T is expanded as

$$T = T_0 + \epsilon^{1-n}T_1 + \dots \quad (3.2)$$

where $0 < n < 1$.

As per the scaling, the Prandtl number is of order $O(\epsilon^{-n})$, the Froude number Fr and the second-grade parameter K are of order $O(1)$, the surface tension parameter S is of order $O(\epsilon^2)$, and the capillary number Ca is of order $O(1)$.

Substituting the expansions (3.1) and (3.2) in the dimensionless model equations (2.15)-(2.23), the *leading order* equations are

$$\frac{\partial u_0}{\partial x} + \frac{\partial w_0}{\partial z} = 0, \quad (3.3)$$

$$-\frac{\partial p_0}{\partial x} + \frac{\partial^2 u_0}{\partial z^2} = 0, \quad (3.4)$$

$$-\frac{\partial p_0}{\partial z} = 0, \quad (3.5)$$

$$-\frac{\partial^2 T_0}{\partial z^2} = 0 \quad (3.6)$$

The corresponding boundary conditions are

$$\text{at } z = h(x, t) : \quad p_0 = 0, \quad \frac{\partial u_0}{\partial z} = 0, \quad \frac{\partial T_0}{\partial z} = -BT_0; \quad (3.7)$$

$$\text{at } z = 0 : \quad u_0 = U(x), \quad w_0 = 0, \quad T = \theta(x) \quad (3.8)$$

Using the stream function $\psi_0 = zU(x)$ the solution of the leading order problem is

$$u_0 = U, \quad w_0 = -zU_x, \quad p_0 = 0, \quad T_0 = \left(\frac{1 + B(h-z)}{1 + Bh} \right) \theta(x). \quad (3.9)$$

For the next order problem, we first solve the temperature equation. With the results of zeroth-order, the temperature equation at order $O(\epsilon^{1-n})$ reads

$$\frac{\partial T_0}{\partial t} + u_0 \frac{\partial T_0}{\partial x} + w_0 \frac{\partial T_0}{\partial z} = \frac{\partial^2 T_1}{\partial z^2} \quad (3.10)$$

with boundary conditions

$$\text{at } z = 0 : \quad T_1 = 0, \quad \text{and at } z = h(x, t) : \quad \frac{\partial T_1}{\partial z} = -BT_1. \quad (3.11)$$

The solution of (3.10) and (3.11) satisfies

$$T_1 = \frac{U\theta_x}{2} \left\{ z^2 - zh \left(\frac{2+Bh}{1+Bh} \right) \right\} - \left\{ \frac{B^2\theta U_x h}{(1+Bh)^2} + \frac{B(U\theta_x - U_x\theta)}{1+Bh} \right\} \left\{ \frac{z^3}{6} - \frac{zh^2}{6} \left(\frac{3+Bh}{1+Bh} \right) \right\} \quad (3.12)$$

The results (3.12) is similar to the one derived in [24] for the Newtonian fluid.

Using the results of zeroth-order and of order $O(\epsilon^{1-n})$, the final solution of the temperature field reads

$$T = \left(\frac{1+B(h-z)}{1+Bh} \right) \theta(x) + \epsilon Pr \left[\frac{U\theta_x}{2} \left\{ z^2 - zh \left(\frac{2+Bh}{1+Bh} \right) \right\} - \left\{ \frac{B^2\theta U_x h}{(1+Bh)^2} + \frac{B(U\theta_x - U_x\theta)}{1+Bh} \right\} \left\{ \frac{z^3}{6} - \frac{zh^2}{6} \left(\frac{3+Bh}{1+Bh} \right) \right\} \right] \quad (3.13)$$

To close the problem, for the derivation of the free surface equation, we need to solve the first and second order continuity and momentum equations. The *first order* problem reads:

$$\frac{\partial u_1}{\partial x} + \frac{\partial w_1}{\partial z} = 0, \quad (3.14)$$

$$\begin{aligned} & \frac{\partial u_0}{\partial t} + u_0 \frac{\partial u_0}{\partial x} + w_0 \frac{\partial u_0}{\partial z} \\ &= -\frac{\partial p_1}{\partial x} + \frac{\partial^2 u_1}{\partial z^2} + K \left[\frac{\partial^3 u_0}{\partial t \partial z^2} - u_0 \frac{\partial^3 w_0}{\partial z^3} - \frac{\partial u_0}{\partial x} \frac{\partial^2 u_0}{\partial z^2} \right. \\ & \quad \left. + w_0 \frac{\partial^3 u_0}{\partial z^3} - \frac{\partial u_0}{\partial z} \frac{\partial^2 w_0}{\partial z^2} + 2 \frac{\partial w_0}{\partial z} \frac{\partial^2 u_0}{\partial z^2} \right] - M^2 u_0, \end{aligned} \quad (3.15)$$

$$-\frac{\partial p_1}{\partial z} - 2K \frac{\partial u_0}{\partial z} \frac{\partial^2 u_0}{\partial z^2} - Fr = 0 \quad (3.16)$$

with boundary conditions at the free surface $z = h(x, t)$:

$$-p_1 - K \left(\frac{\partial u_0}{\partial z} \right)^2 = Sh_{xx}, \quad (3.17)$$

$$\begin{aligned} & \frac{\partial u_1}{\partial z} + K \left[\frac{\partial^2 u_0}{\partial t \partial z} + u_0 \frac{\partial^2 u_0}{\partial x \partial z} + w_0 \frac{\partial^2 u_0}{\partial z^2} + \frac{\partial u_0}{\partial z} \frac{\partial w_0}{\partial z} \right. \\ & \quad \left. - \frac{\partial u_0}{\partial x} \frac{\partial u_0}{\partial z} - 2h_x \left(\frac{\partial u_0}{\partial z} \right)^2 \right] \\ &= -M_w \left[\frac{\partial T_0}{\partial x} + h_x \frac{\partial T_0}{\partial z} \right] \end{aligned} \quad (3.18)$$

and at the sheet $z = 0$,

$$u_1 = 0, \quad w_1 = 0 \quad (3.19)$$

Using the solution of zeroth order problem, the first order solutions for the velocity and pressure can be found out as follows:

$$u_1 = (UU_x + Frh_x - Sh_{xxx} + M^2U) \left(\frac{z^2}{2} - hz \right) + z\phi(x, t), \quad (3.20)$$

$$\begin{aligned} w_1 &= -\frac{z^3}{6} (UU_x + Frh_x - Sh_{xxx} + M^2U)_x \\ & \quad + \frac{z^2}{2} \frac{\partial}{\partial x} [h(UU_x + Frh_x - Sh_{xxx} + M^2U) - \phi(x, t)] \end{aligned} \quad (3.21)$$

$$p_1 = Fr(h - z) - Sh_{xx} \quad (3.22)$$

We introduce for brevity the notation $\phi(x, t) = -M_w \left(\frac{\theta}{1+Bh} \right)_x$ and $f(x, t) = UU_x + Frh_x - Sh_{xxx} + M^2U$.

The model equations for *second order* problem for velocity and pressure are:

$$\frac{\partial u_2}{\partial x} + \frac{\partial w_2}{\partial z} = 0, \quad (3.23)$$

$$\begin{aligned} & \frac{\partial u_1}{\partial t} + u_0 \frac{\partial u_1}{\partial x} + u_1 \frac{\partial u_0}{\partial x} + w_0 \frac{\partial u_1}{\partial z} + w_1 \frac{\partial u_0}{\partial z} \\ &= -\frac{\partial p_2}{\partial x} + \frac{\partial^2 u_0}{\partial x^2} + \frac{\partial^2 u_2}{\partial z^2} \\ &+ K \left[\frac{\partial^3 u_1}{\partial t \partial z^2} - u_0 \frac{\partial^3 w_1}{\partial z^3} - u_1 \frac{\partial^3 w_0}{\partial z^3} - \frac{\partial u_0}{\partial x} \frac{\partial^2 u_1}{\partial z^2} \right. \\ &- \frac{\partial u_1}{\partial x} \frac{\partial^2 u_0}{\partial z^2} + w_0 \frac{\partial^3 u_1}{\partial z^3} + w_1 \frac{\partial^3 u_0}{\partial z^3} - \frac{\partial u_0}{\partial z} \frac{\partial^2 w_1}{\partial z^2} - \frac{\partial u_1}{\partial z} \frac{\partial^2 w_0}{\partial z^2} \\ &\left. + 2 \frac{\partial w_0}{\partial z} \frac{\partial^2 u_1}{\partial z^2} + 2 \frac{\partial w_1}{\partial z} \frac{\partial^2 u_0}{\partial z^2} \right] - M^2 u_1, \end{aligned} \quad (3.24)$$

$$-\frac{\partial p_2}{\partial z} + \frac{\partial^2 w_0}{\partial z^2} + K \left[-2 \frac{\partial u_0}{\partial z} \frac{\partial^2 u_1}{\partial z^2} - 2 \frac{\partial u_1}{\partial z} \frac{\partial^2 u_0}{\partial z^2} \right] = 0 \quad (3.25)$$

with boundary conditions at $z = h(x, t)$

$$-p_2 + 2 \left(-h_x \frac{\partial u_0}{\partial z} + \frac{\partial w_0}{\partial z} \right) + K \left(-2 \frac{\partial u_0}{\partial z} \frac{\partial u_1}{\partial z} \right) = 0, \quad (3.26)$$

$$\begin{aligned} & \frac{\partial w_0}{\partial x} + \frac{\partial u_2}{\partial z} - h_x^2 \frac{\partial u_0}{\partial z} + 2h_x \left(\frac{\partial w_0}{\partial z} - \frac{\partial u_0}{\partial x} \right) \\ &+ K \left[\frac{\partial^2 u_1}{\partial t \partial z} + u_0 \frac{\partial^2 u_1}{\partial x \partial z} + u_1 \frac{\partial^2 u_0}{\partial x \partial z} + w_0 \frac{\partial^2 u_1}{\partial z^2} + w_1 \frac{\partial^2 u_0}{\partial z^2} + \frac{\partial u_0}{\partial z} \frac{\partial w_1}{\partial z} \right. \\ &\left. + \frac{\partial u_1}{\partial z} \frac{\partial w_0}{\partial z} - \frac{\partial u_0}{\partial x} \frac{\partial u_1}{\partial z} - \frac{\partial u_1}{\partial x} \frac{\partial u_0}{\partial z} + 2h_x \left(-2 \frac{\partial u_0}{\partial z} \frac{\partial u_1}{\partial z} \right) \right] = 0, \end{aligned} \quad (3.27)$$

and at $z = 0$, i.e.

$$u_2 = 0, \quad w_2 = 0 \quad (3.28)$$

Using the solution of the zeroth-order and first-order problem, the second order problem satisfies

$$\begin{aligned} u_2 &= \left(\frac{z^4}{24} - \frac{h^3 z}{6} \right) g_1(x, t) + \left(\frac{z^3}{6} - \frac{h^2 z}{2} \right) g_2(x, t) + \left(\frac{z^2}{2} - hz \right) g_3(x, t) \\ &+ z \left[U_{xx} h + 4U_x h_x + K f(h_t + U h_x + U_x h) \right. \\ &\left. + K (-\phi_t - U \phi_x + 2U_x \phi) \right], \end{aligned} \quad (3.29)$$

$$\begin{aligned} w_2 &= \left(-\frac{z^5}{120} + \frac{h^3 z^2}{12} \right) \frac{\partial g_1}{\partial x} + \frac{z^2 h^2 h_x}{4} g_1 + \left(-\frac{z^4}{24} + \frac{h^2 z^2}{4} \right) \frac{\partial g_2}{\partial x} \\ &+ \frac{z^2 h h_x}{2} g_2 + \left(-\frac{z^3}{6} + \frac{h z^2}{2} \right) \frac{\partial g_3}{\partial x} + \frac{z^2}{2} h_x g_3 - \frac{z^2}{2} \frac{\partial}{\partial x} \left[U_{xx} h \right. \\ &\left. + 4U_x h_x + K f(h_t + U h_x + U_x h) + K (-\phi_t - U \phi_x + 2U_x \phi) \right], \end{aligned} \quad (3.30)$$

$$p_2 = -2U_x, \quad (3.31)$$

where $g_1(x, t) = f_t + Uf_x - U_x f + M^2 f$, $g_2(x, t) = -(h_t + Uh_x + M^2 h)f - hf_t - Uhf_x + \phi_t + U\phi_x + M^2 \phi$, and $g_3(x, t) = -3U_{xx} - K(f_t + Uf_x - 3U_x f)$.

4. THIN FILM EQUATION

Using the kinematic boundary condition, the free surface evolution equation can be obtained as follows:

$$h_t + \frac{\partial}{\partial x} F(h) = 0, \tag{4.1}$$

where

$$\begin{aligned} F(h) = & Uh + \epsilon \left(-\frac{h^3 f}{3} + \frac{h^2 \phi}{2} \right) + \epsilon^2 \left[\frac{-3h^5}{40} (f_t + Uf_x - U_x f + M^2 f) \right. \\ & - \frac{5h^4}{24} (-fh_t - f_t h - Uhf_x - Uh_x f + \phi_t + U\phi_x + M^2 \phi - M^2 fh) \\ & - \frac{h^3}{3} \left(-3U_{xx} - Kf_t - KUf_x + 3KU_x f \right) + \frac{h^2}{2} (U_{xx} h + 4U_x h_x \\ & \left. + Kf(h_t + Uh_x + U_x h) + K(-\phi_t - U\phi_x + 2U_x \phi) \right] \end{aligned}$$

with $\phi(x, t) = -M_w \left(\frac{\theta}{1+Bh} \right)_x$ and $f(x, t) = UU_x + Frh_x - Sh_{xxx} + M^2 U$.

The closure of the thin film equation requires the boundary condition for the film height. At the origin, we apply the symmetry boundary condition which imposes that the gradient of the field variable h and its higher derivatives must vanish i.e.

$$h_x = 0, \quad h_{xxx} = 0, \quad h_{xxxx} = 0. \tag{4.2}$$

At the other end of the domain, we assume that the same sheet stretching rate continues beyond the computed domain. We also assume that the gradient of the free surface extends out of the computational domain. These boundary conditions are consistent with those mentioned in [9, 26]. Finally, the model equation is supported by the initial condition $h(x, 0) = 1 + \delta(x)$.

5. NUMERICAL SOLUTION

The transient film thickness (4.1) with supportive boundary and initial conditions are solved using finite volume method. In this paper, we mostly follow the finite volume technique described in Sellier et al. [25, 19] on a uniform grid system with implicit flux discretization.

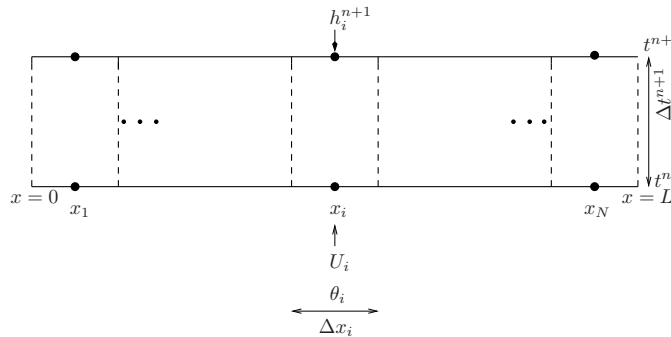


FIGURE 2. Typical grid used for the finite volume discretization

As shown in Figure (2), we discretized the fluid domain using a uniform grid system. The unknown variable h and the known fields U and θ are located at the cell centers. The flow domain $[0, L]$ is discretized into N equal size grid cells of size $\Delta x_i = L/N$, and define $x_i = \Delta x_i/2 + (i - 1)\Delta x_i$, $i = 1, 2, \dots, N$, so that x_i is the center of the cell. The numerical solution is evaluated at the discrete time levels t^n , $n = 0, 1, 2, \dots$ with time step $\Delta t^{n+1} = t^{n+1} - t^n$. From the given cell averaged solution h_i^n over the cell $[x_i, x_{i+1}]$, the solution at the next time step t^{n+1} is obtained by integrating (4.1) over the space and time intervals $[x_i, x_{i+1}] \times [t^n, t^{n+1}]$ which gives the discretized equation:

$$(h_i^{n+1} - h_i^n)\Delta x_i + (F_{i+1/2}^{n+1} - F_{i-1/2}^{n+1})\Delta t^{n+1} = 0 \quad (5.1)$$

for nodes $i = 1, 2, \dots, N$, where the discrete flux function is

$$F_{i+1/2}^{n+1} = F(x_{i+1/2}, t^{n+1}). \quad (5.2)$$

For the internal nodes, the face values are evaluated using linear interpolation from nodal values and gradients using central differences such as

$$\begin{aligned} h(x_{i+1/2}, t^{n+1}) &= \frac{1}{2} (h_{i+1}^{n+1} + h_i^{n+1}), \\ h_x(x_{i+1/2}, t^{n+1}) &= \frac{1}{\Delta x_i} (h_{i+1}^{n+1} - h_i^{n+1}) \end{aligned}$$

Similarly, for other terms, we can derive the expressions like for the second, third and fourth order derivative terms

$$\begin{aligned} h_{xx}(x_{i+1/2}, t^{n+1}) &= \frac{1}{\Delta x_i^2} (h_{i+1}^{n+1} - 2h_i^{n+1} + h_{i-1}^{n+1}), \\ h_{xxx}(x_{i+1/2}, t^{n+1}) &= \frac{1}{\Delta x_i^3} (h_{i+2}^{n+1} - 3h_{i+1}^{n+1} + 3h_i^{n+1} - h_{i-1}^{n+1}), \\ h_{xxxx}(x_{i+1/2}, t^{n+1}) &= \frac{1}{\Delta x_i^4} (h_{i+3}^{n+1} - 4h_{i+2}^{n+1} + 6h_{i+1}^{n+1} - 4h_i^{n+1} + h_{i-1}^{n+1}) \end{aligned}$$

The boundary nodes at the origin are discretized using boundary conditions (4.2) and at the other end of the domain; we assume that the same sheet temperature profiles and the sheet stretching rate continues beyond the computed domain. We also assume that the gradient of the free surface extends out of the computational domain.

Equation (5.1) describes an implicit time discretization scheme. Since the governing equation is nonlinear, a system of nonlinear algebraic equations needs to be solved at each time step. The MATLAB *fsolve* routine is used for this purpose. This routine uses a non-linear least-squares algorithm to solve a system of non-linear equations. A good initial starting guess is required to solve the nonlinear equations. A reasonable initial guess for the free surface is chosen to be unity throughout the discrete domain at the first time step. Therefore, the disturbance function to the initial film thickness $\delta(x)$ is considered to be zero throughout the discussion. The solution from the previous time step can be used otherwise. Convergence is usually achieved in less than ten iterations, and the convergence criterion is that the norm of the residuals should be less than 10^{-7} .

6. RESULTS AND DISCUSSION

In this section some simulation results of free surface profiles and the temperature distribution at the free surface are presented at different times and for the different flow parameters. In Figure (3) the free surface profiles are given at different times with variation of the second-grade non-Newtonian parameter. The left panel results are for the fixed Hartmann number $M = 2$ and the right panel are for $M = 4$. The other parameters used for the simulations are mentioned in the figure caption. By comparing the left and right panels of Figure (3) we can see that with increasing Hartmann number M the fluid thinning behavior slows down due to the effect of the Lorentz force. It is further clear that the free surface height is decreasing with increasing time. Again with increasing second-grade parameter the film thinning behavior decreases. This is due to the fact that for the higher value of K , the tensile stress between fluid layer is higher and consequently higher resistance to motion which decreases the rate of film thinning.

The effect of Marangoni number M_w on the free surface profile is described in the left panel of Figure (4). The sinusoidal temperature profile $\theta(x) = 0.6 + 0.5 \sin(2\pi x/10)$ (right panel of Figure (4)) is imposed at the sheet and the linear stretching velocity $U = 0.1x$ is considered. The free surface profiles at two different times are given for different values of M_w with the variation of the second-grade parameter K . It is clear from Figure (4) that the thermocapillary deforms the free surface and this deformation is advected downstream by stretching velocity. The Marangoni number that characterizes the relation between the temperature dependent surface tension and viscous forces. The high Marangoni number means the lower the viscous forces and thereby the fluid moves faster and the thinning rate increases. It can also be observed that the thinning rate is faster near the origin for lower value of viscoelastic parameter.

The effect of stretching velocity on film height is discussed next. The temperature profile $\theta(x) = 1 - e^{-x^2/33}$ was imposed on the sheet and the following three different stretching velocity distribution is considered:

$$\begin{aligned} U(x) &= 0.6(0.1x + 0.01x^2), && \text{(parabolic concave),} \\ U(x) &= 0.1x, && \text{(linear),} \\ U(x) &= 0.75(1 - (0.1x - 1)^2), && \text{(parabolic convex).} \end{aligned} \tag{6.1}$$

The free surface profiles are given at a fixed time $t = 10$ (non-dimensional). The results confirm that the parabolic concave stretching velocity profile makes the film thinner away from the origin. It is further observed that influence of second grade parameter decelerate the film thinning behaviour of the fluid.

To explore the effect of stretching rate on the free surface profile with variation of second-grade parameter, the finite volume scheme was run for the two different linear stretching velocity, i.e., $U = \eta x$ where $\eta \in \{0.05, 0.1\}$, and varying the values of K from $K = 0$ to $K = 10$ with an increment of five. The free surface profile is plotted in Figure (6) at a fixed time $t = 10$ (non-dimensional) for different stretching speed with different values of K . For $U = \eta x$ where $\eta = 0.1$, the rapid stretching of the film will result in the rapid build-up of stresses. Clearly, the faster the stretching, the faster the thinning of the fluid. The larger the viscoelastic parameter K , the larger the departure from the purely viscous case ($K = 0$) because the additional stresses the fluid needs to overcome the flow.

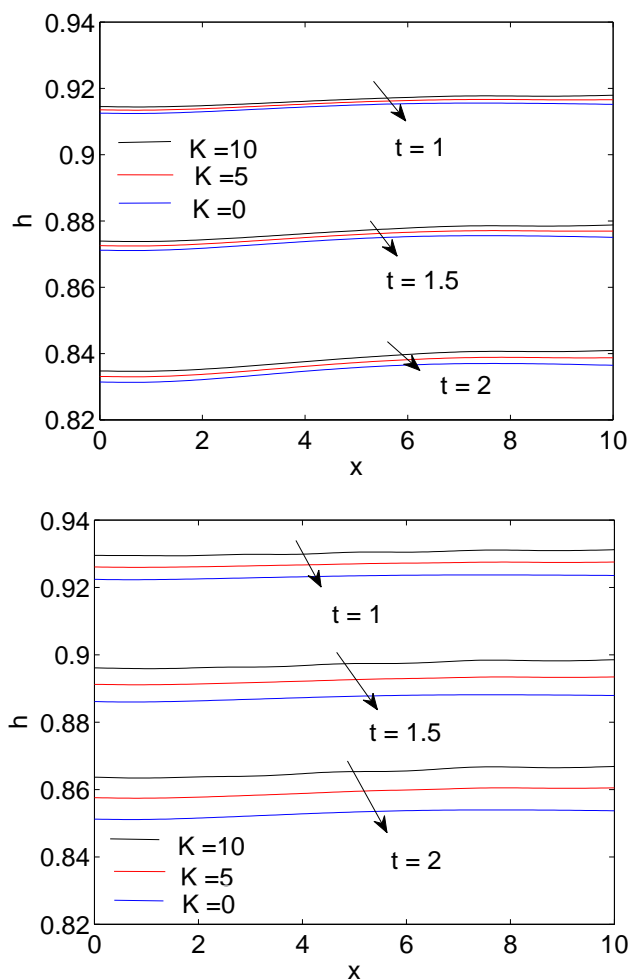


FIGURE 3. Film thickness profile for $S = 2$, $Fr = 2$, $B = 1$, $M_w = 2$, $\epsilon = 0.1$ with $U = 0.1x$, and $\theta(x) = e^{-x^2/33}$, left: Hartmann number $M = 2$, right: Hartmann number $M = 4$

The effect of Biot number on the temperature profile at the free surface of the thin film is demonstrated in Figure (7). The temperature profile at the fluid-gas interface is given at two different times with variation of Biot number (B). The Biot number, that compares the relative magnitudes of resistances to internal conduction and surface convection. In a high Biot number flow, the surface convection dominates the internal conduction and consequently the rate of heat transfer to the fluid through the sheet is higher. Moreover, temperature increases with increase of time as film thins faster (right panel of Figure (7)). We have observed that the Biot number has no significant effect on the thinning behavior of the fluid.

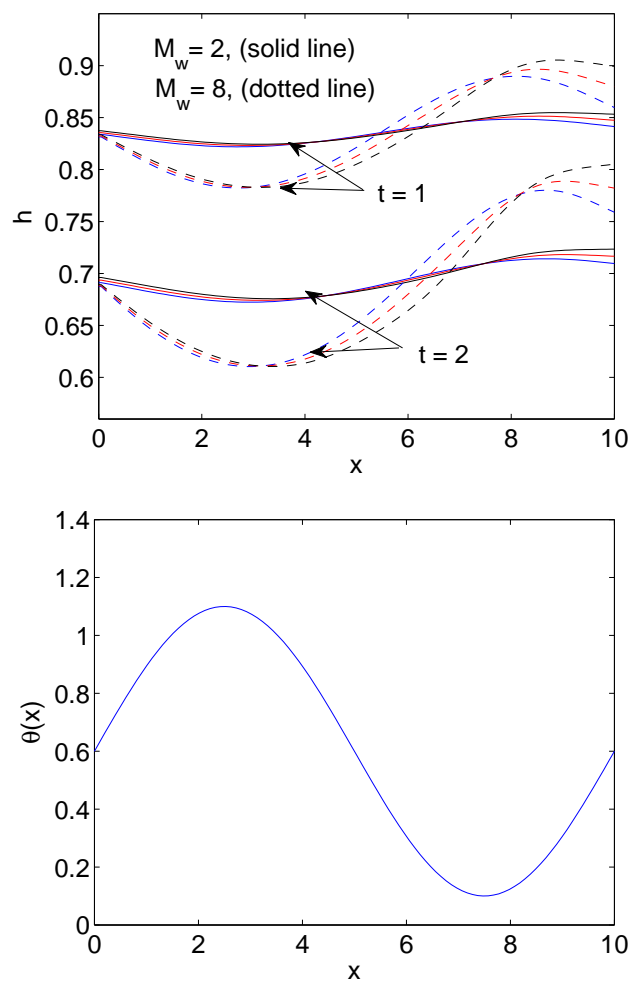


FIGURE 4. Film thickness profile for $S = 2$, $Fr = 2$, $B = 1$, $M = 2$, $\epsilon = 0.1$ with $U = 0.1x$, left: Film thickness profile ($K = 0$ (blue curve), $K = 5$ (red curve), $K = 10$ (black curve)), right: Corresponding temperature profile $\theta(x) = 0.6 + 0.5 \sin(2\pi x/10)$

Conclusion. A model for the dynamics of thin film over the heated steady stretching sheet under the uniform transverse magnetic field is derived based on the long-wave theory. The derivation of the numerical scheme for the unsteady free surface model by finite volume method and their simulations for the wide range of parameters provides a deeper understanding of the film thinning process of the non-Newtonian second-grade fluid. The numerical solution reveals the dependency of the film thinning behavior on the stretching rate and the second-grade fluid parameter. Moreover, the film thinning rate is influenced by the thermocapillary forces and magnetic parameter. It is hoped that the desired film thickness can be achieved by controlling the flow parameters. Future work will explore the derivation of free

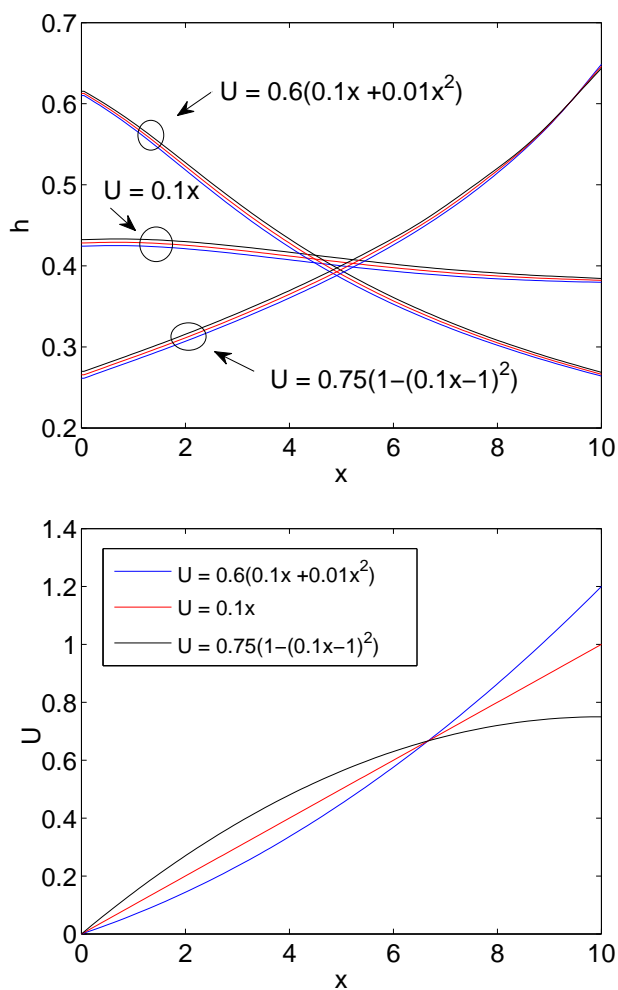


FIGURE 5. Results for the different stretching velocity profile with temperature profile $\theta(x) = 1 - e^{-x^2/33}$ with $S = 2$, $Fr = 2$, $B = 1$, $M = 2$, $M_w = 8$, $\epsilon = 0.1$ at time $t = 10$ (non-dimensional), left: Film thickness profiles ($K = 0$ (blue curve), $K = 5$ (red curve), $K = 10$ (black curve)), right: Corresponding stretching velocity profiles

surface model for the dynamics of film thickness in a similar flow geometry for a third-grade non-Newtonian fluid.

REFERENCES

- [1] H. I. Andersson, J. B. Aarseth, N. Braud, B. S. Dandapat; Flow of a power-law fluid film on an unsteady stretching surface, *J. of Non-Newtonian Fluid Mechanics*, 62(1) (1996), 1–8.
- [2] H. I. Andersson, J. B. Aarseth, B. S. Dandapat; Heat transfer in a liquid film on an unsteady stretching surface, *Int. J. Heat Mass Transfer*, 43 (2000), 69–74.

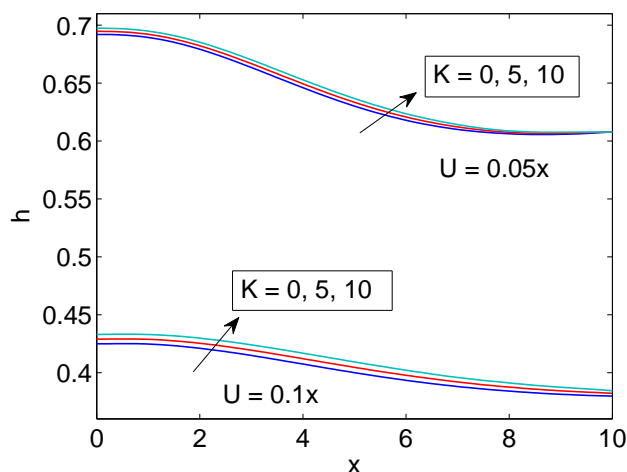


FIGURE 6. Effect of stretching rate and viscoelastic parameter K on free surface profile with $S = 2$, $Fr = 2$, $B = 1$, $M = 2$, $M_w = 8$, $\epsilon = 0.1$ at time $t = 10$ (non-dimensional) with $\theta(x) = 1 - e^{-x^2/33}$

- [3] R. C. Aziz, I. Hashim; Liquid film on unsteady stretching sheet with general surface temperature and viscous dissipation, *Chin. Phys. Lett.*, 27 (2010), 110202.
- [4] I.-Chung Liu, H. I. Andersson; Heat transfer in a liquid film on an unsteady stretching sheet, *Int. J. Therm. Sci.*, 47 (2008), 766–772.
- [5] B. S. Dandapat, A. Kitamura, B. Santra; Transient film profile of thin liquid film flow on a stretching surface, *Zeitschrift fur angewandte Mathematik und Physik ZAMP*, 57(4) (2006), :623–635.
- [6] B. S. Dandapat, S. Maity; Flow of a thin liquid film on an unsteady stretching sheet, *Physics of Fluids*, 18(10) (2006), Article ID 102101, 7 pages.
- [7] B. S. Dandapat, B. Santra, H. I. Andersson; Thermocapillarity in a thin liquid film on an unsteady stretching surface, *Int. J. Heat and Mass Transfer*, 46 (2003), 3009–3015.
- [8] B. S. Dandapat, B. Santra, K. Vajravelu; The effects of variable fluid properties and thermocapillarity on the flow of a thin film on an unsteady stretching sheet, *Int. Jr. Heat and Mass Transfer*, 50 (2007), 991–996.
- [9] B. S. Dandapat, S. K. Singh; Thin film flow over a heated nonlinear stretching sheet in presence of uniform transverse magnetic field, *Int. Commu. in Heat and Mass Transfer*, 38(3) (2011), 324–328.
- [10] J. E. Dunn, R. L. Fosdick; Thermodynamics, stability and boundedness of fluids of complexity 2 and fluids of second grade, *Arch Ration Mech Anal.*, 56(3) (1974), 191–252.
- [11] J. E. Dunn, K. R. Rajagopal; Fluids of differential type critical review and thermodynamics analysis, *Int. Jr. Eng Sci.*, 33:689–747, 1995.
- [12] R. L. Fosdick, K. R. Rajagopal; Anomalous features in the model of second order fluids. *Arch Ration Mech Anal.*, 70:145–152, 1979.
- [13] T. Hayat, S. Saif, Z. Abbas; The influence of heat transfer in an MHD second grade fluid film over an unsteady stretching sheet, *Physics Letters A*, 372(30) (2008), 5037–5045.
- [14] T. Hayat, M. Sajid; Analytic solution for axisymmetric flow and heat transfer of a second grade fluid past a stretching sheet, *Int. J. of Heat and Mass Transfer*, 50(1) (2007), 75–84.
- [15] R. Levy, D. B. Hill, M. G. Forest, J. B. Grotberg; Pulmonary fluid flow challenges for experimental and mathematical modeling. *Integrative and Comparative Biology*, 54(6) (2014), 985–1000.

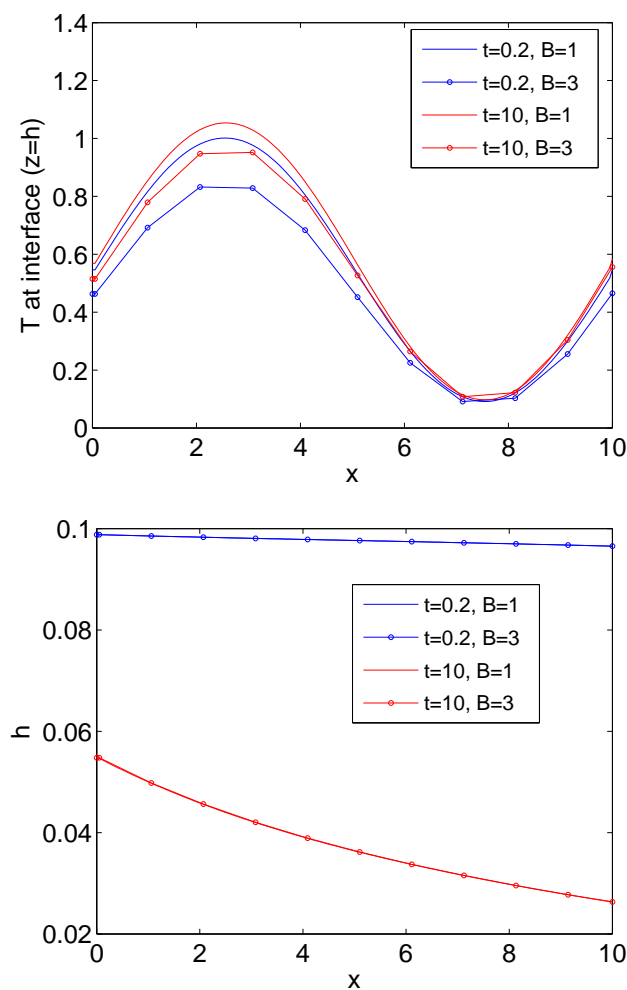


FIGURE 7. Variation of temperature profile at the interface ($z = h$) for different Biot number B for $S = 2$, $Fr = 2$, $K = 1$, $M = 2$, $M_w = 2$, $\epsilon = 0.1$, $Pr = 1$ with $U(x) = 0.6(0.1x + 0.01x^2)$ and $\theta(x) = 0.6 + 0.5 \sin(2\pi x/10)$, left: temperature profiles at the interface, right: corresponding free surface profiles

- [16] Y. Khan, Q. Wu, N. Faraz, A. Yildirim; The effects of variable viscosity and thermal conductivity on a thin film over a shrinking/stretching sheet, *Comp. Math. Appl.*, 61 (2011), 3391–3399.
- [17] F. Md. Ali, R. Nazar, N. Md.Arifin, I. Pop; MHD boundary layer flow and heat transfer over a stretching sheet with induced magnetic field, *Heat and mass Transfer*, 47(2) (2011), 155–162.
- [18] N. F. M. Noor, I. Hashim; Thermocapillary and magnetic field effects in a thin liquid film on an unsteady stretching surface, *Int. Jr. Heat Mass Transfer*, 53 (2010) 2044–2051.
- [19] S. Panda, M. Sellier, M. C. S. Fernando, M. K. Abeyratne; Process parameter identification in thin film flows driven by a stretching surface, *Int. Jr. of Engineering Mathematics*, Article ID 485431, 2014.

- [20] R. S. Rivlin, J. L. Ericksen; Stress deformation relations for isotropic materials, *J. Ration Mech. Anal.*, 4 (1955), 323–425.
- [21] M. Sajid, I. Ahmad, T. Hayat, M. Ayub; Unsteady flow and heat transfer of a second grade fluid over a stretching sheet, *Comm. in Nonlinear Science and Numerical Simulation*, 14(1) (2009), 96–108.
- [22] M. Sajid, T. Hayat; Influence of thermal radiation on the boundary layer flow due to an exponentially stretching sheet, *Int. Comm. in Heat and Mass Transfer*, 35(3):347–356, 2008.
- [23] M. Z. Salleh, R. Nazar, I. Pop; Boundary layer flow and heat transfer over a stretching sheet with Newtonian heating, *J. of the Taiwan Institute of Chemical Engineers*, 41(6) (2010), 651–655.
- [24] B. Santra, B. S. Dandapat; Unsteady thin-film flow over a heated stretching sheet, *Int. Jr. of Heat and Mass Transfer*, 52 (2009), 1965–1970.
- [25] M. Sellier, S. Panda; Surface temperature reconstruction based on the thermocapillary effect, *The ANZIAM Journal*, 52:146–159, 2010.
- [26] S. K. Singh, B. S. Dandapat; Thin film flow of Casson liquid over a non-linear stretching sheet in the presence of a uniform transverse magnetic field, *Canadian Journal of Physics* 93 (2015), 1067–1075.
- [27] B. Wang; Liquid film on an unsteady stretching surface, *Quart. Appl. Math.*, 48 (1990), 601–610.

KIRAN KUMAR PATRA

DEPARTMENT OF MATHEMATICS, NATIONAL INSTITUTE OF TECHNOLOGY CALICUT, NIT(P.O)-673601, KERALA, INDIA

E-mail address: kirankumarpatra1984@gmail.com

SATYANANDA PANDA (CORRESPONDING AUTHOR)

DEPARTMENT OF MATHEMATICS, NATIONAL INSTITUTE OF TECHNOLOGY CALICUT, NIT(P.O)-673601, KERALA, INDIA

E-mail address: satyanand@nitc.ac.in

MATHIEU SELLIER

DEPARTMENT OF MECHANICAL ENGINEERING, UNIVERSITY OF CANTERBURY, PRIVATE BAG 4800, CHRISTCHURCH 8140, NEW ZEALAND

E-mail address: mathieu.sellier@canterbury.ac.nz